Department of Science and Technology

Engineering Research and Development for Technology (ERDT) Consortium

Science Education Institute

Criticality Analysis of Component Plants In Bioenergy-based Symbiotic Network

Michael Francis D. Benjamin[1,2,*], Raymond R. Tan[1] and Luis F. Razon[1]

[1] *Chemical Engineering Department*
De La Salle University, 2401 Taft Avenue, 1004 Manila, Philippines
[2] *Chemical Engineering Department*
University of Santo Tomas, España Blvd., 1006 Manila, Philippines
**Corresponding Author: michael_benjamin@dlsu.edu.ph*

Abstract

The production of ethanol from 1st generation renewables still faces criticisms with regards to its sustainability. Through industrial symbiosis (IS), the efficiency and environmental performance of a bioethanol plant can be enhanced. However, due to the increased interdependence of component plants in such symbiotic network, cascading failure may occur when one plant is unable to run at full capacity that will result in a deviation from a baseline configuration. This work further extends criticality analysis, originally developed for polygeneration plants, to a bioenergy-based symbiotic network. The component plants in the entire network can then be ranked based on criticality index. Such information can be used for developing risk mitigation measures, such us planning for system redundancy. A case study is presented to demonstrate how the method determines the criticality index of component plants in a bioenergy-based symbiotic network.

Introduction

The utilization of 1st generation biofuels is being confronted by several sustainability issues such as the creation of "carbon debt" due to land conversion (Fargione et al., 2008) and significant greenhouse gas emissions (Börjesson, 2009). The efficiency and environmental performance of a bioethanol plant can be enhanced through industrial symbiosis (IS) by creating a bioenergy-based symbiotic network (Gonela and Zhang, 2014). IS seeks to create synergistic product, by-product, and utility exchanges among separate component plants in order to achieve sustainable operations (Chertow, 2000).

However, due to the increased interdependence of component plants within a symbiotic network, there will be a cascading effect in the entire system when one plant becomes inoperable. In this work, the concept of criticality index is further extended to quantify the effects of a plant's failure within a bioenergy-based symbiotic network. The component plants in the entire network can then be ranked based on this index to determine which facilities are critical.

Industrial networks can be modelled using Input-Output (IO) analysis (Khanna and Bakshi, 2009). IO models are used to quantify the robustness and risks associated with economic, environmental, and energy systems (Tan et al., 2012; Haimes and Jiang, 2001).

Problem Statement

- Assume each *nth* component plant produces a particular *nth* product stream
- Given a % capacity reduction of a component plant
- Determine the Criticality Index of the component plants
- Rank the component plants based on the criticality index

Criticality Index Derivation

$$\mathbf{A}\mathbf{x} = \mathbf{y} \quad (1)$$

$$\begin{bmatrix} \mathbf{0} & \mathbf{A}' \\ -\mathbf{I} & \mathbf{A}'' \end{bmatrix} \begin{bmatrix} \mathbf{y}'' \\ \mathbf{x}' \end{bmatrix} = \begin{bmatrix} \mathbf{B}' & \mathbf{I} \\ \mathbf{B}'' & \mathbf{0} \end{bmatrix} \begin{bmatrix} \mathbf{x}'' \\ \mathbf{y}' \end{bmatrix} \quad (2)$$

$$\mathbf{c} = (\mathbf{y_o}'' - \mathbf{y_n}'')\hat{\mathbf{y}}_\mathbf{o}''^{-1} \quad (3)$$

$$\mathbf{z} = \mathbf{c}\hat{\mathbf{x}}_\mathbf{o}^{-1} \quad (4)$$

where,
Eq. (1) – BBIS network input-output (IO) model, demand-driven
Eq. (2) – Plant capacity perturbation IO-based model
Eq. (3) – Criticality column vector, fractional change in output stream
Eq. (4) – Criticality index column vector

Case Study: Bioenergy-based Symbiotic Network

The hypothetical design of the bioenergy-based symbiotic network shown in Figure 1 comprises the following component plants: Bioethanol plant (BIO), Combined Heat and Power plant (CHP), Malt plant (MP), Anaerobic Digestion plant (AD), and a Cement plant (CP). These production plants are designed to produce the following main product streams: Bioethanol (E), Power (P), Malt (M), Biogas (G), and Cement (C).

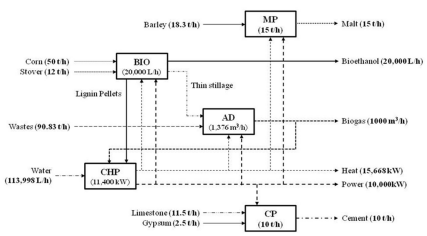

Figure 1. Bioenergy park input and output flow diagram for the baseline state.

Table 1. Process data for the baseline state of the bioenergy park.

Product Stream	BIO	CHP	MP	AD	CP	Final Output
Bioethanol, L/h	1	0	0	0	0	20,000
Power, kW	-0.00022	1	-10	-0.36	-75	10,000
Malt, t/h	0	0	1	0	0	15
Biogas, m^3/h	0	-0.033	0	1	0	1,000
Cement, t/h	0	0	0	0	1	10

Table 2. Sizing of component plants for the baseline state.

	BIO, L/h	CHP, kW	MP, t/h	AD, m^3/h	CP, t/h
Plant Capacity	20,000	11,400	15	1,376	10

Results

Equation (1) is used to solve the baseline capacities of the component plants, shown in Table 2, as well as the stream rates (i.e. product, by-product, and utility). Figure 1 shows the complete baseline state of the symbiotic network. Equation (2) is used to solve the final output of each product stream in each scenario and the fractional change in plant capacity as well as the final output of product streams. Equation (3) is then used to determine the fractional change in the directly affected product streams. Finally, Equation (4) is used to solve the criticality index of the component plants using a plant capacity reduction of 5%. The results of these calculations are presented in Table 3.

Table 3. Fractional Change in Final Output and Criticality Index of Plants.

Plant - Product Stream	c	z	Rank
BIO - Bioethanol	0.050	1.0	3
CHP - Power	0.056	1.13	2
MP - Malt	0.050	1.0	3
AD - Biogas	0.068	1.36	1
CP - Cement	0.050	1.0	3

The bioethanol plant, CHP plant, malt plant, anaerobic digestion plant and cement plant have criticality indices of 1.0, 1.13, 1.0, 1.36 and 1.0 respectively. The component plants in the symbiotic network can then be ranked based on this index to determine which plant will require risk mitigation measures. This index is constant for a given network configuration regardless of the capacity perturbation magnitude. In this work, the anaerobic digestion plant has the highest value of criticality index which means that a reduction in anaerobic digestion plant capacity results to a greater net loss in biogas output compared to other product streams.

Conclusion

A criticality index of component plants for a bioenergy-based symbiotic network was developed in this work. The criticality index is defined as the ratio of the fractional change in the final output of the directly affected product stream based on the baseline state to the fractional change in the capacity of the corresponding component plant. Based on this index, the component plants can be ranked to determine the most critical facility in the network.

References

Börjesson, P. (2009). Good or bad bioethanol from a greenhouse gas perspective – What determines this? Applied Energy, 86, 589–594.

Chertow, M. R. (2000). Industrial symbiosis: Literature and taxonomy. Annual Review of Energy and Environment, 25, 331–357.

Fargione, J., Hill, J., Tilman, D., Polasky, S., & Hawthorne, P. (2008). Land clearing and the biofuel carbon debt. Sciencex press, 1–4.

Gonela, V., & Zhang, J. (2014). Design of the optimal industrial symbiosis to improve bioethanol production. Journal of Cleaner Production, 64, 513–534.

Haimes, Y. Y., & Jiang, P. (2001). Leontief-based model of risk in complex interconnected infrastructures. Journal of Infra structure Systems, 7, 1–12.

Khanna, V., & Bakshi, B.R. (2009). Modeling the risks to complex industrial networks due to loss of natural capital. IEEE International Symposium on Sustainable Systems and Technology. doi:10.1109/ISSST.2009.5156771.

Tan, R. R., Lam, H. L., Kasivisvanathan, H., Ng, D. K., Foo, D. D., Kamal, M., et al. (2012). An algebraic approach to identifying bottlenecks in linear process models of multifunctional energy systems. Theoretical Foundations of Chemical Engineering, 46, 642–650.

Department of Science and Technology

ERDT

DOST Science Education Institute

DESIGN AND IMPLEMENTATION OF FUZZY LOGIC CONTROLLED UNINTERRUPTIBLE POWER SUPPLY INTEGRATING RENEWABLE SOLAR ENERGY

Angelo A. Beltran Jr. and Felicito S. Caluyo
School of Graduate Studies
Mapua Institute of Technology, Manila Philippines
Email: abeltranjr@hotmail.com, fscaluyo@mapua.edu.ph

ABSTRACT
The control and operation of electronic systems relies and depends on the availability of the power supply. Rechargeable batteries have been more pervasively used as the energy storage and power source for various electrical and electronic systems and devices, such as communication systems, electronic devices, renewable power systems, electric vehicles, etc. However, the rechargeable batteries are subjected to the availability of the external power source when it is drained out. Because of the concern of battery life, environmental pollution and a possible energy crisis, the renewable solar energy has received an increasing attention in recent years. A fuzzy logic control based grid tied uninterruptible power supply integrating renewable solar energy can be used for electrical and electronic systems to produce power generation. This paper presents the design and implementation of fuzzy logic control based grid tied uninterruptible power supply integrating the renewable solar power energy system. The uninterruptible power supply (UPS) system is characterized by the rechargeable battery that is connected with the Photovoltaic Panel through the DC/DC converter, the utility AC through the AC/DC converter and the load is connected through the DC/AC converter. The whole operation is controlled by the fuzzy logic algorithm. A complete hardware prototype system model of the fuzzy logic control based on the grid tied uninterruptible power supply integrating with the renewable solar energy is designed and implemented. The operation and effectiveness of the proposed system is then demonstrated by the actual and real time implementation of the fuzzy logic control grid tied operation uninterruptible power supply integrating renewable solar energy connected to the rechargeable battery bank and a PIC microcontroller platform for fuzzy logic control and operation.

KEYWORDS: Fuzzy Logic Control, Solar Energy, Utility AC, Uninterruptible Power Supply

INTRODUCTION

Nearly all electrical power comes from fossil fuels (e.g., coal and oil) and once that these fossil fuels have been burnt; they are gone forever. Burning the fossil fuels creates pollution; this in its turn is having a growing and adverse effect on the regulation of the earth's climate. The more energy people use each day, then the less there is left for the future. There is a worldwide need to reduce the amount of energy consumption, and everybody has his part to play whether in industry, transport, business, construction, or at home. Consuming less energy and being more efficient in the way people run their homes will naturally save money and protect the environment as well. At the same time, it will help protect the environment and safeguard the future. The energy production has become expensive worldwide and its shortage has lead to intensified research studies for developing alternate sources of energy which are clean, pollution free, and eco friendly. Due to the increasing global interest on the conservation of environment, renewable energy systems are gaining attention in the recent years. Advanced solutions must be applied to design and control clean power generation, energy harvesting, and energy storage systems which must then guarantee efficiency, robustness, safety, reliability, and sustainability. Hence, using the electricity wisely is good for the environment which saves money in homes, businesses, and nation's energy supply. One of the many ways of saving and controlling the use of electricity is to have a power supply. Known electronics equipment nowadays including household appliances used power supply in order to operate them. Without the power supply, it is impossible for us to run those appliances. A power supply is a device that supplies electrical energy to one or more electric loads. It may also refer to a device that converts one or another form of energy (e.g., mechanical, chemical, solar) into electrical energy. It is most commonly applied to devices that convert one form of electrical energy into another. In all aspects, every power supply needs an external power for it to run, and every power consumed by its load or electronic circuitry directly attached to it is proportional to the household power consumption, and power consumption is proportional to the bill of payments. Knowing the importance of power supply and its proper application can truly help conserved energy.

OBJECTIVES OF THE STUDY

(a) To design a fuzzy logic controller (FLC) for the uninterruptible power supply integrating solar energy with a power from the utility company.
(b) To build and construct a prototype incorporating the solar energy source, utility AC source, and fuzzy logic controller for uninterruptible power supply.
(c) To design the AC/DC converter for the utility AC source, the DC/DC converter for solar energy source, and the DC/AC converter for the load
(d) To test the performance of the system.

METHODOLOGY

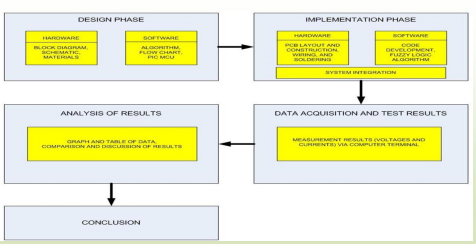

The conceptual framework of this study comprises of the following namely the PV Panel, DC/DC, DC/AC, AC/DC converter, Fuzzy Logic Controller, Data logging via RS-232C serial interface and, LCD display The use of the battery allows the photovoltaic system to behave as a real source to the feeder so that it may exhibit constant voltage levels to the different loads.

CONCEPTUAL FRAMEWORK

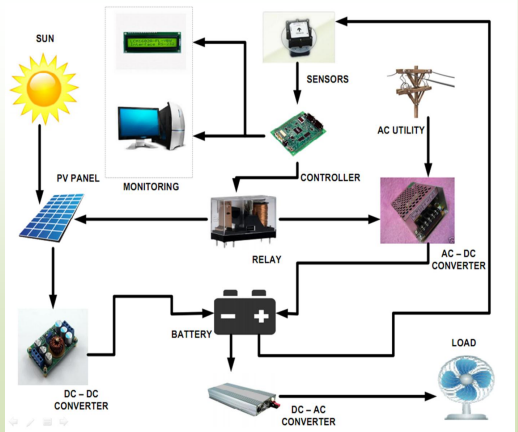

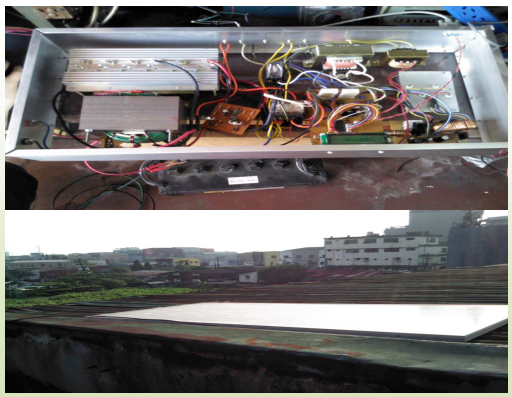

RESULTS

Table 1: Data and measurement results during system test.

Date	Time	Solar Voltage	DC/DC Voltage	Battery Voltage	Charge Current	Load Current	AC Inv. Vout
11/1/2013	8:20AM	19.5 V	14.3 V	11.2 V	2.4 A	2.2 A	157 V
11/1/2013	3:20PM	18.9 V	14.2 V	11.1 V	2.3 A	2.1 A	158 V
11/2/2013	9:30AM	18.7 V	14.1 V	11.3 V	2.2 A	2.2 A	159 V
11/2/2013	4:30PM	18.2 V	14.1 V	11.1 V	2.1 A	2.0 A	157 V
11/3/2013	7:30AM	18.3 V	14.1 V	11.2 V	2.1 A	2.0 A	160 V
11/3/2013	3:54PM	18.6 V	14.2 V	11.2 V	2.2 A	2.1 A	159 V
11/4/2013	8:30AM	19.2 V	14.2 V	11.9 V	2.2 A	2.1 A	160 V
11/4/2013	3:30PM	19.1 V	14.2 V	11.9 V	2.4 A	2.0 A	158 V
11/5/2013	7:20AM	19.0 V	14.1 V	12.1 V	2.2 A	2.2 A	160 V
11/5/2013	1:25PM	18.9 V	14.2 V	12.8 V	2.2 A	2.1 A	159 V
11/5/2013	4:00PM	18.9 V	14.1 V	13.3 V	2.2 A	2.1 A	159 V
11/6/2013	10:00AM	18.7 V	14.2 V	12.0 V	2.1 A	2.0 A	158 V
11/6/2013	3:27PM	18.4 V	14.2 V	11.9 V	2.1 A	2.0 A	158 V
	Average	18.8 V	14.2 V	11.8 V	2.2 A	2.1 A	158.6 V

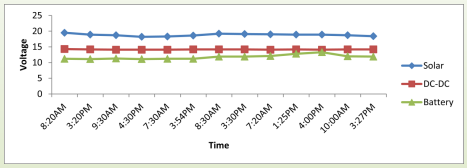

Figure 1: Voltage vs Time measurement results.

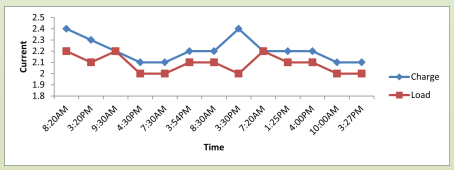

Figure 2: Current vs Time measurement results.

CONCLUSION

A clean renewable source of energy is a challenging problem for electrical and electronic devices nowadays to provide uninterrupted electric power supply for continuous operation. This paper has presented a novel design and implementation of fuzzy logic control based grid tied uninterruptible power supply integrating environment friendly renewable solar energy. The proposed system utilizes the clean source of energy, which is solar and converts to electrical energy to facilitate the charging operation of the battery through the DC/DC converter and generates a constant active uninterruptible power supply to the load under normal runtime operating conditions. The system through fuzzy logic control automatically configures to utility AC in the absence of solar energy for storage demand in charging the battery and providing uninterruptible power supply to the dynamic load. The fuzzy logic control based grid tied uninterruptible power supply integrating with the renewable solar energy has been designed and implemented in a complete hardware prototype model. Results have clearly confirmed that the constructed prototype is remarkably effective as uninterruptible power supply. It significantly provides a smooth and continuous power supply to the electrical load being served with. The system can be easily used as uninterrupted power supply (UPS) for the electrical and electronic devices.

Department of Science and Technology

Science Education Institute

Design of a Methyl Laurate – Methyl Myristate PCM Storage System to Support a Solar Vapor-Compression Chiller

Rommel N. Galvan, Rizalinda R. de Leon & Maria Natalia R. Dimaano

Abstract

Binary mixture containing 80% by volume methyl myristate and 20% methyl laurate was used as phase change material (PCM) for a design to support a generic solar vapor-compression chiller. The experimental melting point and latent heat of the mixture obtained from differential scanning calorimetric analysis (DSC) is 9.8°C and 215.24kJ·kg^{-1}, respectively. A shell and tube heat exchanger design was employed to hold 44.5 kg of the PCM mixture. A 20-footer intermodal container van was used to simulate a controlled room.

A laboratory chiller and PCM heat exchanger were used by the system to cut off the peak room temperature to 2°C during day time. The system has been proven to be economical for it lowered the energy requirement of the chiller to attain human comfort. The PCM system increased the coefficient of performance (COP) of the chiller from 7.8 to 14.2 during day time operations.

Introduction

In the past decade, the economic situation started to change because of the rising energy prices. The energy demand that ensures a comfortable environment for humans in buildings has increased worldwide and especially the use of electricity for cooling and air-conditioning is rising fast. Cooling and air-conditioning often cause a peak in electricity demand in afternoon hours when, just because of that, peak electricity prices apply.

Current researches now focus on phase change material (PCM) because of their ability to control both temperature and heat absorption. These properties, with the aid of proper engineering may create usable equipment for low temperature energy storage, lowering the energy requirement of existing cold water chiller systems for small to medium sized cooling duties. The main focus of this study is to develop a PCM system to lower the existing energy requirement of a cooling system without compromising human comfort.

Objectives of the Study

(1) Design a cooling apparatus utilizing a PCM previously developed (Galvan, 2010).

(2) Create a simulated environment to test and examine the equipment, and

(3) Determine if the human comfort requirements (Çengel, 2003) is achievable.

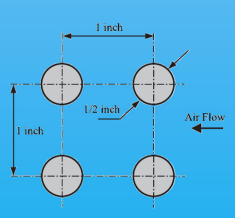

Figure 1, Piping cross section

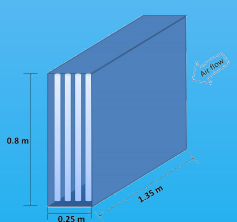

Figure 2, PCM Box schematic

Methodology

PCM System

A rectangular box of size 1.35 m (length) x 0.25 m (width) x 0.8 m (height) was used to house 477 aluminum tubes (12.7 mm, ½ inch nominal tubing). The size of the rectangular box will allow 9 by 53 tubes using the arrangement described in figure 1. The box was thermally insulated using 50 mm Styrofoam™, with both the 0.25 x 0.8 faces torn off to allow air flow through the equipment (figure 2).

PCM mixture of 80% by volume methyl myristate (MM) and 20% methyl laurate (ML) was used to fill the tubes. A total of 44.5 kg was used for this setup. A Toshiba Machine LT DK70 is used as the water chiller for the setup. A fabricated evaporator with two cooling fans was attracted to this chiller, which was attached to the back of the PCM box.

Simulated Environment

A 20 footer container van was used to simulate a room. The van was insulated from the inside by 50 mm Styrofoam™, and the outside wall was painted flat white. Two (2) thermocouples were placed, one 1 meter away from the outside wall of the van, the other within the dead center of the van. Temperatures were logged using Fluke Hydra 2635A. The evaporator and the PCM box was placed inside the van with the chiller placed outside. Two (2) insulated 1 inch copper pipes connect the chiller with the evaporator. The operation of the fan and the chiller was controlled using a thermostat. The chiller was also controlled during PCM charging hours.

Results

Differential scanning calorimetry (DSC) suggest that the 80/20 MM-ML mixture has a melting point just below 10°C making it applicable for low temperature energy storage (figure 3). Furthermore, the enthalpy of fusion of 215 kJ/kg makes the mixture suitable for storage control (Mehling, 2007)

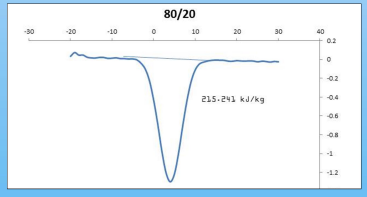

Figure 3, DSC thermogram of 80/20 volume percent methyl myristate – methyl laurate

Initial test using the simulated room from 12MN April 26 to 12MN April 29 suggests that the chiller + PCM setup cuts the peak temperature by about 2 to 3 Celsius degrees as shown in figure 4. During the daytime test, the chiller is programed to operate at a lower heat duty (30°C condenser, 10°C evaporator) than the normal setup of 40°C condenser, 5°C evaporator (figure 5).

The coefficient of performance (COP) running the water chiller alone to lower the room temperature by 3 Celsius degrees (left of figure 5) is:

$$\frac{273+5}{40-5} = 7.8$$

Running the chiller with the PCM, the COP (right of figure 5) is:

$$\frac{273+10}{30-10} = 14.2$$

The actual cooling capability of 44.5 kg PCM is 44.5 x 215.24 = 9578.18 kJ which is equivalent to running the water chiller alone for about 2.5 hours

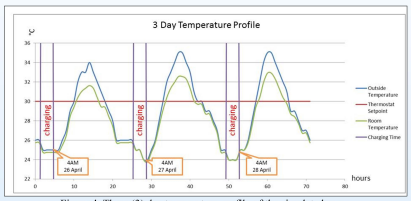

Figure 4, Three (3) day temperature profile of the simulated room

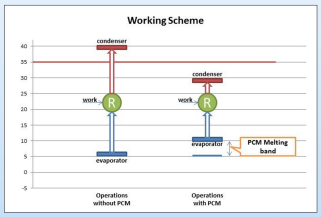

Figure 5, working scheme of the water chiller during normal operations (left) and with PCM (right)

Conclusion

The experiment setup proves the feasibility of using a PCM with a melting point of below 10°C to be used as a temperature controlled accessory to lower the energy requirements of a conventional water chiller for room space cooling. There is a significant increase in the coefficient of performance of the chiller from its normal operating condition, than that of the system which included the PCM mix. Furthermore, the use of the PCM mix cuts the time needed to operate the water chiller to perform space cooling for the simulated room.

Recommendation

The initial test concentrated only on the discharge phase of the chiller-PCM setup. The authors will need to determine if there are significant effects on the space cooling capability of the system if the charging phase were altered or optimized.

Furthermore, the study focuses on the attainment of human comfort levels with respect to space cooling. Cabeza, Mehling, Hiebler, and Ziegler (2002) discussed the parameters to attain human comfort as the temperature of the room, the room air speed and the humidity. For this part of the study, the room air speed and humidity were both unaccounted for and is assumed to be constant throughout the experiment procedures. Next phase will focus on these parameters one at the time.

References

Cabeza, L. F., Mehling, H., Hiebler, S., & Ziegler, F. (2002). Heat transfer enhancement in water when used as PCM in thermal energy storage. Applied Thermal Engineering, 22(10), 1141-1151.

Çengel, Y. A. (2003). Heat Transfer: A Practical Approach: McGraw-Hill.

Galvan, R., de Leon, R, & Dimaano, M. N. (2010). Estimation of Enthalpy of Fusion of Methyl Laurate Paper presented at the 5th ERDT Conference, Manila.

Mehling, H., Cabeza, L. (2007). Phase Change Materials and their Basic Properties.

Department of Science and Technology

Department of Science Education Institute

Development of a Mechanical Windpump for Supplemental Irrigation

Roejae Carlo A. ANG, Rossana Marie C. AMONGO, Delfin C. SUMINISTRADO, Ronaldo B. SALUDES

ABSTRACT

With the continuous threat on fuel shortage, wind energy is considered harnessing to prime agricultural activities. While numerous types of windmills are already available in the market, there is a growing interest and need of wind energy extraction systems with other blade shapes and structural configurations.

This paper aims to develop a mechanical windpump for supplemental irrigation. Relevant design criteria such as functionality and simplicity in construction, installation and operation are considered in the design phase. The use of a low speed Savonius wind turbine in combination to a high speed Centrifugal pump in a purely mechanical transmission is studied to meet design criteria. The use of a scale model for the wind turbine based on similitude is employed. The Savonius turbine is designed with a rotor diameter of 41 cm and rotor height of 61.5 cm so as to fit the size of an existing wind tunnel. The wind turbine is subjected to varying wind speed in the wind tunnel which is simulated from the actual wind regime of the installation site. Wind turbine characteristics such as cut-in, cut-out and rated wind speed, circumferential velocity of the rotor, tip-speed ratio, etc. are recorded. Using a predicting equation and a length scale n, the data are used to predict the power and torque that can be produced by the actual prototype. The torque predicted is generated using a variable-speed motor for the testing of the Centrifugal pump on a separate test rig. The pump discharge at varying speed is recorded. Analysis on the effect of wind speed on system efficiency is done using CRD.

INTRODUCTION

Importance of Freshwater Pumping

- Water involved in agriculture is significant and most of it is provided directly by rainfall. However, rainfall variability and seasonal variation limits the potential of rain to substantially meet agricultural demands.
- Freshwater withdrawal provides the option of supplying the vast need.
- The Food and Agriculture Organization (FAO 2012) reported that agriculture accounts for 70% of water consumption at a world level.
- In the Philippines, 85% of the water demand goes to agriculture. A large portion of this total water consumption is acquired from lakes, rivers, man-made and natural reservoirs.

Importance of Using Windmill for Water Pumping

- Another feasible method that can be employed is pumping out groundwater. With clear anticipation of rising global concerns on climate change and fuel shortage, researchers around the world proposed the integration of renewable energy sources with water pumping (Gopal et. al. 2013).
- Wind energy is a promising source for water pumping since it is clean, free, and reliable. When the critical wind speeds exceed 3 m/s wind pumps are usually competitive with photovoltaics and diesel system, depending on the cost of fuel (Kristoferson and Bolkalders 1986).As there is a growing interest and need of wind energy extraction systems, other blade shapes and structural configurations are expected to come out. However, the characteristic behaviors of some of these windmills are still unknown and they have yet to undergo tests for proper performance evaluation.

Figure 1. Windpump

Source: http://www.edupic.net/Images/Science/wind_power_well_pump01.JPG

OBJECTIVES

- To assess the wind and ground water profile of the site selected for potential installation
- To design and construct a mechanical windpump system
- To test the characteristics and performance of the windpump in a laboratory under a simulated environment

METHODOLOGY

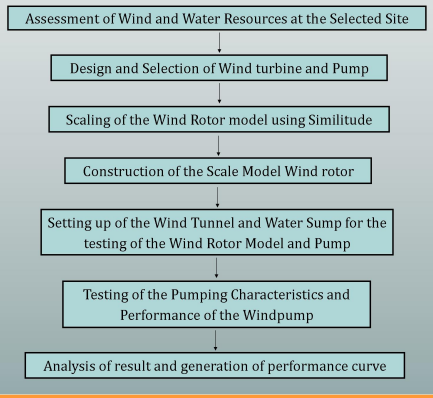

RESULTS

*Analysis of the wind speed data for six months are shown in the two figures below. Wind speed reading is still going on at present.

- 6.25 m/s of hourly wind speed prevails 73% of the time*
- The lowest recorded wind speed of 3.5 m/s is relatively higher than the usual cut-in wind speed of most wind turbines
- For a one square meter of wind rotor projected area, wind power of the selected site is calculated to be 150 Watts
- For the designed scale model, the power is 37.7 Watts at 6.25 m/s wind speed
- Testing of the scale model wind rotor and pump are still on going

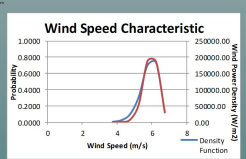

Figure 2. Graph of the Probability Density Function of the wind Speed Distribution and Wind Power Density against Wind Speed

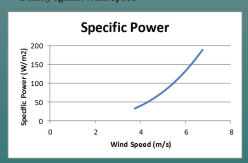

Figure 3. Graph of the Specific Power of the Site

Acknowledgement

University of the Philippines—Los Baños

Department of Science and Technology (ERDT)

DESIGN CONCEPT

Wind Turbine

- Since the windmill to be designed will be used for water pumping, the first requirement it must meet is the starting torque.
- A two-bladed Savonius wind turbine was chosen since it has good torque characteristic. It is also simple to construct and maintain despite its relatively low Cp.

Table 1. Summary of Design Parameters

Parameters	Value
Number of Blade	2
Aspect Ratio	1.5
Rotor Height	61.5 cm
Rotor Diameter	41 cm
Shaft Diameter	1.9 cm
Chord Length	19.55 cm
Swept Area	2521.5 cm²
Solidity	1.907
Overlap	0.95 cm
Cup Radius	11.2 cm

Pump

- The wind pump system to be designed will provide supplemental irrigation water (large volumes in low heads).
- The selection of pump will be based on the dimensionless pump characteristic called specific speed Ω.
- A 1x1 centrifugal pump is used. Though centrifugal pump is next only to reciprocating or piston pump in terms of common use, it still has advantages in certain circumstances. It can operate at <10m heads and has high flow to head ratio (Ford et. al. 2013).

Similitude Requirements

From Khan (1978), the power derived from a Savonius Wind rotor is a function of:

Table 2. Pertinent variables for Savonius Wind Rotor analysis

Symbol	Description of Quantity	Dimensions
P	Shaft power	$MLT^{-2} \cdot L \cdot T^{-1}$
d	Width of the maximum projection of the rotor	L
S	Projected area of the rotor	L^2
ρ	Density of the flowing fluid	ML^{-3}
γ	Kinematic viscosity of flowing fluid	L^2T^{-1}
g	Acceleration due to gravity	LT^{-2}
V	Velocity of flowing fluid	LT^{-1}
U	Circumferential velocity of the outermost point of the rotor	LT^{-1}
T	Shaft torque	$MLT^{-2} \cdot L$

Employing the Buckingham Pi Theorem and Dimensional Analysis, the following relationship and predicting equations are derived:

$$V_m = \frac{V_p}{\sqrt{n}} \qquad T_p = n^4 T_m \qquad P_p = n^{7/2} P_m$$

FIELD TEST OF THERMOELECTRIC GENERATOR USING PARABOLIC TROUGH SOLAR CONCENTRATOR FOR POWER GENERATION

Rommel R. VIÑA[1], Kenneth S. LIMPAHAN[1], Feliciano B. ALAGAO, Ph.D.[1]
[1]MSU-Iligan Institute of Technology, Bonifacio Ave., Iligan City

ABSTRACT

A 2.65 square meter effective area parabolic trough solar concentrator was fabricated. On the focal line is a blackened copper collector plate which served as high temperature heat reservoir of eight 40mm x 40mm thermoelectric modules. The modules dissipated heat through a rectangular tube with coolant inlet temperature maintained at around 28°C by a coolant loop with a direct contact cooling tower.

Collector temperature was also kept below the 125°C module maximum operating temperature by adjusting the effective area by controlling the exposed area of the reflector.

Using a dummy load, preliminary tests indicated voltage readings of as high as 15 vdc and current readings of up to 192 mA, all with 8 modules in series and 30% of reflector area. A steady voltage of 12 vdc was achieved with the use of a voltage regulator.

Overall results showed the potential of TEG and solar energy in power generation.

INTRODUCTION

The typical solar trough power system utilize the solar radiation concentrated by the trough collector to heat a flowing fluid, such as oil or molten salt, to a temperature enough to produce steam. Then the steam produced is used to drive a steam turbine that drives an electric generator to produce electricity. A thermoelectric generator (TEG) is a thermoelectric module (TEM) that is used to generate electricity as heat from a high temperature source is allowed to flow through the thermoelectric module down to the low temperature sink.

This study evaluated the use of TEMs in a solar trough for electric power generation.

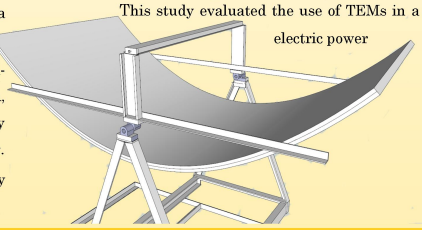

OBJECTIVES

- Design and fabricate a motorized-tracking 4-ft x 8-ft surface area solar trough
- Design and fabricate a liquid-cooled concentrated solar receiver/collector with eight thermoelectric modules sandwiched.
- Evaluate the electricity generated versus the temperature difference across the modules.
- Evaluate the electricity generated versus the concentration ratio and solar irradiance.
- Evaluate the actual generation efficiency

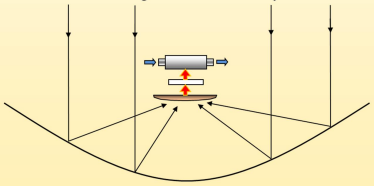

METHODOLOGY

Fabrication and configuration of solar trough, heat dissipation system (HDS), and collector/receiver assembly

↓

Configuration of instruments and data logging system

↓

Starting the HDS, the solar tracking, and the data acquisition and logging system

↓

Manual uncovering and adjustment of concentrator reflector exposed area (to keep the collector temperature below 125°C)

↓

Shutting down and unloading of logged data

↓

Data analysis, interpretation and presentation

RESULTS

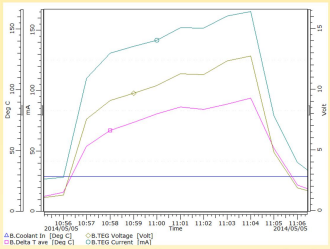

Figure 1. Profile of electricity generated and temperature difference between collector and coolant [May 5 data]

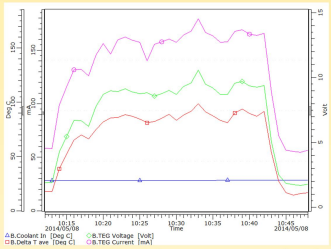

Figure 2. Profile of electricity generated and temperature difference between collector and coolant [May 8 data]

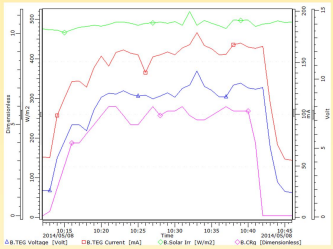

Figure 3. Profile of electricity generated, concentration ratio and irradiance [May 8 data]

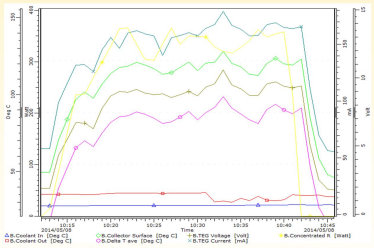

Figure 4. Profile of electricity generated, temperatures and computed concentrated radiation [May 8 data]

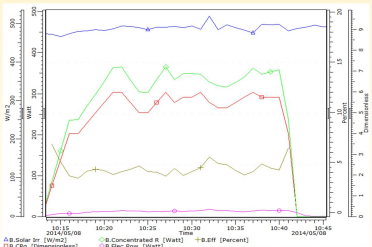

Figure 5. Profile of irradiance, power generated, concentrated solar radiation and efficiency [May 8 data]

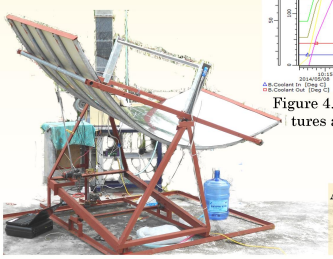

CONCLUSIONS

- The thermoelectric modules (TEMs) did convert the solar energy into electrical energy.
- The eight TEMs in series can generate up to 15 Volts
- The eight TEMs in series can also generate up to 21 Watts (at 12.7 Volts and 165 mA current)
- There is potential of thermoelectric generator (TEG) and solar energy in power generation

RECOMMENDATIONS

- The use of TEMs with higher operating temperatures
- Automation in reflector exposed area control
- More robust solar tracking system

Acknowledgements
- Department of Science and Technology
- ERDT Consortium
- MSU-IIT College of Engineering
- Prof. & Mrs. E. P. Villanueva, Ph.D.

Further Information:
rommel_vina@yahoo.com
+63-919-202-0294

Department of Science and Technology

Science Education Institute

OPTIMIZATION AND SITE SELECTION OF LOW HEAD MICROHYDRO SYSTEM INSTALLATION FOR ELECTRICITY GENERATION

Elisa R. SAN JUAN[1], Rossana Marie C. AMONGO[2], Delfin C. SUMINISTRADO[3], and Ronaldo B. SALUDES[4]

[1] Assistant Professor, University of the Philippines Rural High School, College of Arts and Sciences, University of the Philippines Los Baños

[2] Assistant Professor, [3] Professor, Institute of Agricultural Engineering, College of Engineering and Agro-industrial Technology, University of the Philippines Los Baños

ABSTRACT

The system of a low head microhydro system installed on irrigation canal for electricity generation was analysed in this study. It incorporated two factors: the draft tube and speed ratio. The maximum power (86.9W) is generated by the modified draft tube of 760 mm length at 13° cone angle with 209 mm intake and 368 mm exit diameters, and speed ratio of 3:8. The most efficient system (31.7%) is the original draft tube of 1000 mm length at 10° cone angle with 215 mm intake and 374 mm exit diameters, and speed ratio of 3:8. The optimum power is produced by the design with original draft tube at speed ratio of 3:8. The microhydro system costs Php 91,362.00. Almost half of the cost, Php 45,774.00, was spent for the labor cost, and Php 45,588.00 was spent for the materials. The cost can be further reduced if fabrication of components is through mass production. Six irrigation canals were characterized and all are suitable for microhydro system installation in terms of head and volumetric flow rate. In the community's acceptability, the microhydro system is accepted by 46% of the respondents however only one person is willing to spend money for the installation.

INTRODUCTION

The world faces serious energy and environmental problems. The current energy supply depends mainly on fossil energy carriers. According to the Renewable Energy Focus Handbook, coal, petroleum and natural gas are by far today's most popular fossil fuels. These fuels need thousands of years to form and huge amount of these has already been consumed in the 20th century. With the ever increasing excessive usage of these fossil energy carriers, future extraction will be more difficult, risky and expensive. As of 2006, there are no practical and available alternative to fossil fuels for most energy needs, so they are still heavily used. Among the renewable energy sources is water. Water energy is the energy derived from the power of water in motion. There are plenty of large hydropower plants operating nowadays. Although it is known that using water as a source of power does no harm to the environment, the installation of the plant facilities have great environmental impacts.

OBJECTIVES

The general objective of the study is to optimize the working conditions of a low-head, turbine-type microhydro system for electricity generation.

The specific objectives are as follows:

1. to determine the optimum operating conditions of the turbine-type microhydro system for electricity generation;
2. to match the type of the energy converter suited for the microhydro system;
3. to calculate for the overall cost of the microhydro system;
4. to identify selected irrigation canals as potential sites for the installation of the microhydro system within Sta. Cruz River Irrigation Systems in Laguna, Philippines;
5. and to determine the community's acceptability of the microhydro system installed on an irrigation canal;

MATERIALS AND METHODS

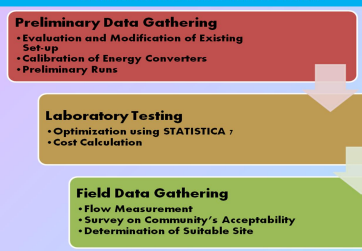

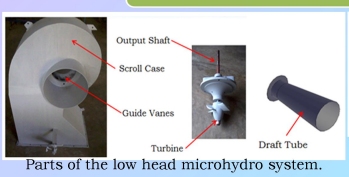

Parts of the low head microhydro system.

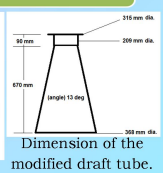

Dimension of the modified draft tube.

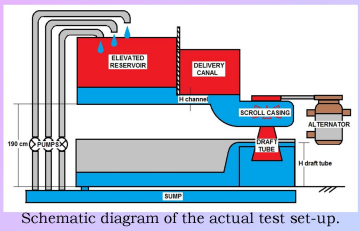

Schematic diagram of the actual test set-up.

Instruments and tools used in the study.

RESULTS

Power generation and efficiencies of the three batches of test runs.

DRAFT TUBE SETTING	SPEED RATIO	ACTUAL POWER (W)	THEORETICAL POWER (W)	TRANSMISSION EFFICIENCY (%)	CONVERSION EFFICIENCY (%)
Design A	3:8	72.8	234.9	97.7	31.7
	1:4	60.9	250.9	92.0	26.4
	3:16	61.8	248.4	95.2	26.1
Design B	3:8	52.6	406.3	96.2	13.7
	1:4	23.4	584.4	91.9	4.7
	3:16	39.2	639.9	90.7	6.8
Design C	3:8	86.9	390.04	94.1	23.8
	1:4	52.0	401.7	97.8	13.2
	3:16	48.0	510.1	94.9	9.9

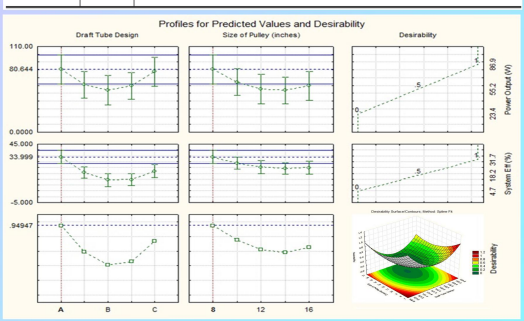

Profiles for predicted values and desirability.

Canal locations, codes, and dimensions.

Canal location	Code	Head (cm)	Width (cm)	Depth (cm)
End of supply canal at Bubucal, Laguna	A	85.0	120.0	15.0
Side of Hanging Bridge, Liliw, Laguna	B	110.0	200.0	10.0
End of Malinao Creek, Laguna	C	90.0	100.0	10.0
Check at Brgy. Mojon, Liliw, Laguna	D	110.0	130.0	20.0
Side of AgriTech Building, Sta. Cruz, Laguna	E	95.0	200.0	50.0
Check at Banca-Banca, Victoria, Laguna	F	112.0	192.0	11.0

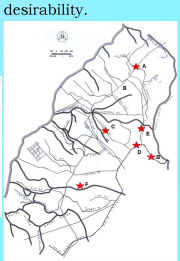

The sites for flow characterization in SCRIS.

Suitability of canals for microhydro system installation.

Canal Code	Water Velocity (m/s)	Width (cm)	Depth (cm)	Volumetric Flow Rate (m^3/s)	Suitability for Installation yes	no
A	0.715	120	15	0.129	√	
B	2.368	200	10	0.474	√	
C	1.319	100	10	0.132	√	
D	1.729	130	20	0.449	√	
E	1.692	200	50	1.692	√	
F	0.578	192	11	0.122	√	

Cost of the microhydro system.

Part	Material Cost (Php)	Labor Cost (Php)
Turbine Component	21,811.00	39,774.00
Canal Component	16,022.00	5,000.00
Electrical Component	7,755.00	1,000.00
Total Cost	**45,588.00**	**45,774.00**

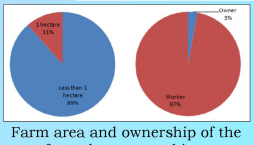

Farm area and ownership of the farm they are working.

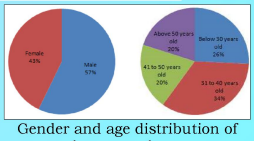

Gender and age distribution of the respondents.

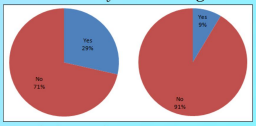

Knowledge and awareness on water power and microhydro system.

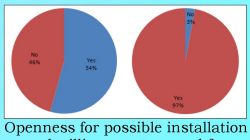

Openness for possible installation and willingness to spend for microhydro system.

RECOMMENDATIONS

The study had obtained the minimum requirements to achieve the objectives. Though, for better results, the system should be tested on field. The conducted laboratory test is not an enough basis for the characterization of the microhydro system. It is better if the system is installed on irrigation canals to clearly see the application of the system.

REFERENCES

BUDYNAS–NISBETT.2006. Shigley's Mechanical Engineering Design .McGraw-Hill.

DA ROSA, A. V. 2005. Fundamentals of Renewable Energy. United States of America. Elsevier Academic Press.

DULAWAN, L. D. 2011. Development of a Turbine for Low Head Microhydroelectric Power Systems. MSAE Thesis. UPLB.

HEINLOTH, K. 2006. Energy Technologies. Renewable Energy. Germany. Springer-Verlag Berlin Heidelberg.

QUASCHNING, V. 2005 . Understanding Renewable Energy Systems. UK. Carl Hanser Verlag GmbH & Co KG.

SAN JUAN, E. R. 2012. Design Modification and Optimization of Low Head Microhydro System for Electricity Generation. MSAE Thesis. UPLB.

SCHLAGER, W. and J. **WEISBLATT**. 2006. Alternative Energy. Vol. 3. China. Thomson Gale.

SHEPERD, W. and D. W. **SHEPERD**. 2003. Energy Studies. 2nd ed. Singapore. Imperial College Press.

SOMMERS, G. L. 2009. Renewable Energy Focus Handbook. United States of America. Elsevier Academic Press.

RESEARCH POSTER PRESENTATION | 2014 ERDT CONGRESS

POWER OUTPUT OPTIMIZATION OF DYE-SENSITIZED SOLAR CELL WITH Fe-Ni CODOPANT, TiO_2 PHOTO-ANODE AND CARBON NANOTUBE AS COUNTER ELECTRODE

Barongan, N. M., Auresenia, J.L.

Chemical Engineering Department, De La Salle University-Manila, 2401 Taft Avenue, Malate, Manila, Philippines

Department of Science and Technology (DOST)

Introduction

- Renewable energy sources (Figure 1) have been eyed on nowadays as alternatives for power generation—that is why researches on developing new methods to convert solar energy to a useful form has a high impact to the modern society where fossil fuels are forecasted to be critically depleted in many years to come.

Figure 1. Examples of Renewable Energy Applications[1]
(from left to right) Wind, Solar, Geothermal, Biofuels

- Solar cells gain popularity due to the ease of installation and environmental friendliness in terms of operation. Dye-sensitized solar cell (DSSC) (Figure 2) is a new type of solar cell—considered as one of the promising renewable energy device because of inexpensive materials and manufacturing and the potential economic advantage (Grätzel, 2003).

Figure 2. Dye-sensitized Solar Cells[2]

- DSSCs are photogalvanic cells which make use of the principles of optical absorption and charge separation processes to effect conversion of light into electric current.

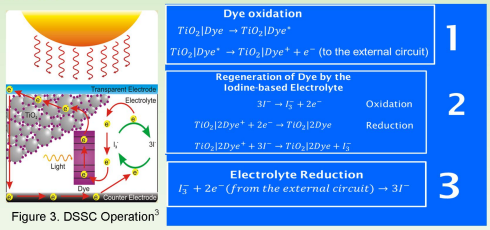

Figure 3. DSSC Operation[3]

- Challenge to DSSC research: **efficiency**
- Most studies focus on studying **only one component** of the cell.
- Intensive studies about **doping applications of the photoanode** in DSSC must be done to know the effect on improving the performance of this kind of solar cell.

Objective

The overall objective of the study is to **optimize the performance of dye-sensitized solar cell by varying iron and nickel dopant ratio, titanium dioxide photanode thickness and carbon nanotube concentration** in three levels using response surface methodology and also to **investigate the correlation/effect of the three factors** with respect to the other components towards achieving maximum power output of the solar cell.

Methodology and Setup

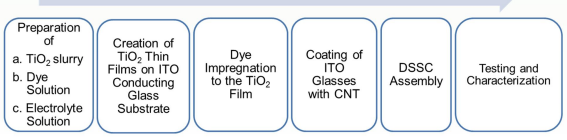

Figure 4. Experimental Procedure

Table 1. Box-Behnken (RSM) Experimental Design

Run	Factor A (Doping Ratio: -1 = Pure Fe, 1 = Pure Ni)	Factor B (TiO2 thick-ness, μm)	Factor C (CNT concentra-tion, mg CNT per 10 mL solvent
1	-1	80	750
2	0	80	500
3	1	40	500
4	0	40	250
5	0	40	750
6	-1	80	250
7	-1	120	500
8	0	80	500
9	1	120	500
10	-1	40	500
11	0	120	750
12	0	120	250
13	0	80	500
14	0	80	500
15	0	80	500
16	1	80	750
17	1	80	250

Figure 5. Fabricated DSSC's

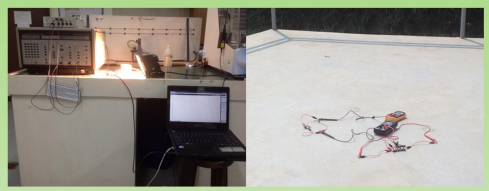

Figure 6. Experimental Setup: artificial light testing (left) and sunlight testing (right)

Results

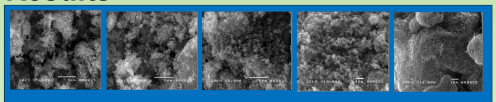

(a) (b) (c) (d) (e)

Figure 7. SEM image of (a) Fe-TiO_2 (b) Fe-Ni-TiO_2 (c) Ni-TiO_2 (d) Pure TiO_2 (e) CNT

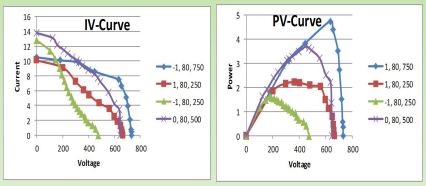

Figure 8. IV-curve and PV-curve for the 4 highest power output DSSC

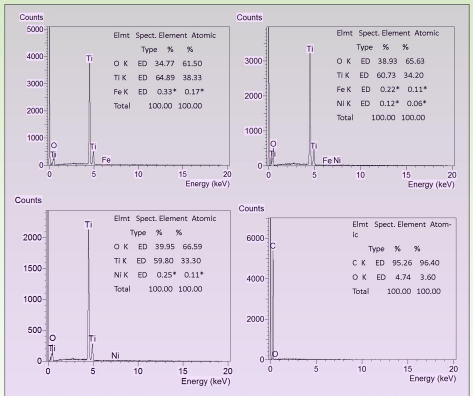

Figure 9. EDX Elemental Composition of (from left to right): Fe-TiO2, Fe-Ni-TiO2, Ni-TiO2, CNT

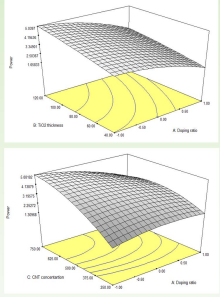

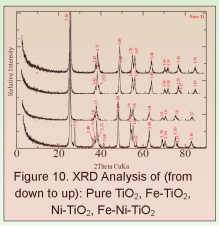

Figure 10. XRD Analysis of (from down to up): Pure TiO_2, Fe-TiO_2, Ni-TiO_2, Fe-Ni-TiO_2

Figure 11. 3D Surface plot for optimum combination of doping ratio, TiO2 thick-jness and CNT concentration

- The 17 fabricated DSSCs were tested using artificial light and sunlight. Based from the optimization done, the actual equation was found to be **$P = 2.607 + 1.19A + 1.270B + 0.796C - 0.406A^2 - 0.0023AB - 0.00278AC + 0.00744BC$.**

Conclusion

A working dye-sensitized solar cell was successfully fabricated and tested using artificial light and sunlight. Based from the optimization done, the optimum setup was found to have a **dopant ratio of 98% Fe - 2% Ni - doped TiO_2, a TiO_2 thickness of 119.22 μm and a carbon nanotube concentration of 722.73 mg per 10 mL solvent**. This combination corresponds to a maximum power output of **5.017 mW**. The maximum efficiency achieved in the experiment was **3.77%**

Recommendation

It is recommended to try other metallic dopants in order to investigate their effects on enhancing the efficiency of DSSC.

References

Bai, Y., Cao, Y., Zhang, J., Wang, M., Li, R., Wang, P., Zakeeruddin, S., & Grätzel, M. (2008). High-performance dye-sensitized solar cells based on solvent-free electrolytes produced from eutectic melts, *Nature Materials*, 7, 626–30.

Chaveanghang, S., Smith, S. M., Sudchanham, J., & Amornsakchai, T. (2011). Enhancement of power conversion efficiency of dye-sensitized solar cells by using multi-walled carbon nanotubes/ TiO_2 electrode, *Journal of the Microscopy Society of Thailand*, 4, 36-40.

Grätzel, M., (2003).Dye-sensitized solar cells. *Journal of Photochemistry and Photobiology* ,4, 145-153.

[1]Images from http://www.sustainable.co.za, http://www.photovoltaic-production.com, http://conserve-energy-future.com and http://sei.oregonstate.edu

[2]Images from http://www.engadget.com and http:/ www.technologyreview.com

[3]Image from http://www.yale.edu